Bifurcation control of the Morris–Lecar neuron model via a dynamic state-feedback control

Le Hoa Nguyen, Keum-Shik Hong & Seonghun Park

Biological Cybernetics
Advances in Computational Neuroscience

ISSN 0340-1200
Volume 106
Number 10

Biol Cybern (2012) 106:587-594
DOI 10.1007/s00422-012-0508-4

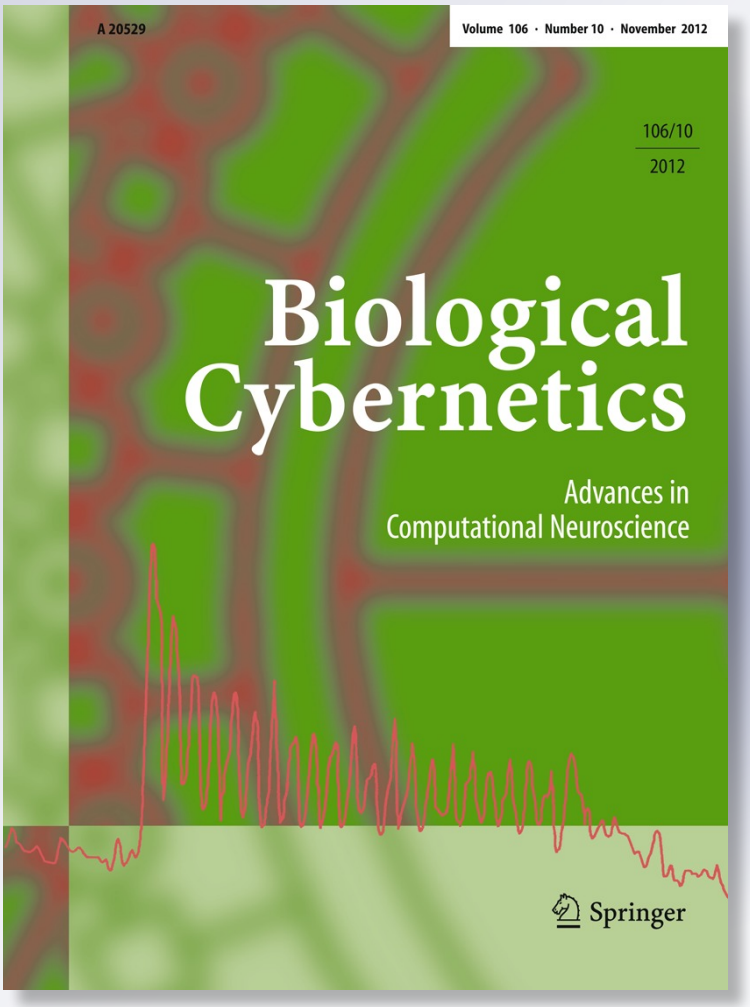

Springer

Biol Cybern (2012) 106:587–594
DOI 10.1007/s00422-012-0508-4

ORIGINAL PAPER

Biological Cybernetics

Bifurcation control of the Morris–Lecar neuron model via a dynamic state-feedback control

Le Hoa Nguyen · Keum-Shik Hong · Seonghun Park

Received: 7 March 2012 / Accepted: 9 July 2012 / Published online: 10 October 2012

Abstract In this paper, we address the control problem of bifurcations in the Morris–Lecar (ML) neuron model. With the use of a dynamic state-feedback control, two Hopf bifurcation points in the ML neuron model with Type II excitability can be relocated to new desired locations simultaneously. Also, with the proposed control law, the neuronal excitability characteristics can be transformed from Type I excitability to Type II excitability by changing the type of bifurcation, in which the neuron goes from quiescence to periodic spiking from a saddle node on an invariant circle bifurcation to a Hopf bifurcation. Simulation results are provided.

Keywords Bifurcation control · Morris–Lecar neuron model · Dynamic state feedback control · Neurological disease · Neuronal excitability

1 Introduction

The nervous system contains a network of neurons that regulate and coordinate all of the physiological processes within our bodies. A breakdown in the coordination and control of the nervous system leads to an abnormality and a disorder in the underlying physiological control mechanism, resulting in the occurrence of many neurological diseases such as, for example, epilepsy, Alzheimer's disease, Parkinson's disease, or schizophrenia (Mackey and an der Heiden 1982; Bélair et al. 1995; Asai et al. 2003). From the viewpoint of nonlinear dynamical systems, these diseases can be considered to be caused by a bifurcation induced by a change in the values of one or more regulating parameters in the relevant nonlinear equations describing the neuronal system (Titcombe et al. 2001; Kramer et al. 2006; Luo et al. 2009). For example, Parkinson's disease constitutes a severe impairment caused by excessive synchronization of neuronal activity in basal ganglia. This excessive synchronization leads to an increase in the amplitude of local field potential oscillations and is considered as the appearance of a Hopf bifurcation of the local field potential (Luo et al. 2009). In the case of epilepsy, Kramer et al. (2006) developed a mathematical model of human cortical electrical activity that can produce activity characteristics of a seizure – a visible symptom of epilepsy. Their model shows that seizurelike oscillations occur when the strength of excitatory synaptic input to both excitatory and inhibitory cortical neurons exceeds a threshold value that induces a Hopf bifurcation in the spatially averaged soma membrane potential of the excitatory cells (Kramer et al. 2006). Therefore, understanding the mechanism leading to a bifurcation of neuronal systems and comprehending the design of a feedback control law by which such bifurcation characteristics could be modified could lead to new diagnostics and therapy trajectories for neurological diseases. For instance, to eliminate seizure activity, a control input can be injected into the human cortex such that it could prevent the occurrence of a Hopf bifurcation in the spatially averaged soma membrane potential of the excitatory cells within a certain range of

L. H. Nguyen · S. Park
School of Mechanical Engineering, Pusan National University, 30 Jangjeon-dong, Gumjeong-gu, Busan 609-735, Republic of Korea
e-mail: nglehoa@pusan.ac.kr

S. Park
e-mail: paks@pusan.ac.kr

K.-S. Hong (✉)
Department of Cogno-Mechatronics Engineering, Pusan National University, 30 Jangjeon-dong, Gumjeong-gu, Busan 609-735, Republic of Korea
e-mail: kshong@pusan.ac.kr

strength of excitatory synaptic input. The objectives of bifurcation control include (1) relocating an inherent bifurcation (Wang and Abed 1995; Yu and Chen 2004; Nguyen and Hong 2012), (2) stabilizing a bifurcated solution or branch (Abed and Fu 1986; Ding and Hou 2010), (3) changing the shape or type of a bifurcation chain (Wang and Abed 1995), and (4) creating a new bifurcation at a preferable parameter value (Abed and Wang 1995; Wen and Xu 2005). Various approaches to bifurcation control have been proposed in the literature including static state feedback (Abed and Fu 1986; Chen et al. 2000; Yu and Chen 2004), dynamic state feedback (Wang and Abed 1995; Nguyen and Hong 2012), time-delayed feedback (Brandt and Chen 1997; Xiao and Cao 2007), harmonic balance approximation (Tesi et al. 1996; Berns et al. 1998), and quadratic invariants in normal forms (Kang 1998).

In a neuronal model, when a parameter changes, for example, an applied current, the neuron can experience a bifurcation – a transition from one qualitative type of dynamic to another. Various types of bifurcation have been reliably observed in neuronal models (Laing and Longtin 2003; Tsumoto et al. 2006; Touboul and Brette 2008; Nguyen and Hong 2011; Lefebvre et al. 2009). Although various electrophysiological mechanisms cause the transition from quiescence to periodic spiking, there are only four types of codimension one bifurcations that a neuronal model typically undergoes, namely, saddle-node bifurcation, saddle-node on invariant circle (SNIC) bifurcation, subcritical Hopf bifurcation, and supercritical Hopf bifurcation. All these bifurcation types have been identified in different models of neurons such as, for example, the Hodgkin–Huxley model, the two-dimensional Hindmarsh–Rose model, the FitzHugh–Nagumo model, the Morris–Lecar (ML) model. (Izhikevich 2000; Brown et al. 2004). Hodgkin (1948) classifies neurons into two types, Type I excitability and Type II excitability. A neuron with Type I excitability exhibits a continuous f–I (the firing frequency versus the applied current) curve that shows the neuron starts firing at an arbitrary low frequency. In contrast, a neuron with Type II excitability exhibits a discontinuous f–I curve, in which the neuron begins firing at a nonzero frequency. From the viewpoint of bifurcation theory, Type I neuronal excitability is observed when the rest potential (quiescent state) disappears through a SNIC bifurcation, while Type II excitability is observed when the rest potential loses stability via a Hopf bifurcation (Rinzel and Ermentrout 1989). Here the Hopf bifurcation can be either subcritical or supercritical.

Recently, it has been reported that a washout-filter-aided dynamic feedback control law can be employed to relocate a bifurcation point and alter the stability of a Hopf bifurcation in neuronal models (Xie et al. 2008a,b; Ding and Hou 2010). The main advantage of using the washout filter is that it preserves the original equilibrium points. However, the filter cannot be applied to systems with two Hopf bifurcations since the relocation of one Hopf bifurcation point affects the location of the other (Xie et al. 2008b). Very recently, we proposed a dynamic state feedback control law that is able not only to relocate two different Hopf bifurcation points simultaneously to any desired locations in n-dimensional nonlinear systems but also to preserve the equilibrium structure of the system (Nguyen and Hong 2012).

In this paper, we pay attention to the control of bifurcations in the ML neuron model. The ML neuron model can exhibit properties of either Type I excitability or Type II excitability when system parameters are set appropriately (Rinzel and Ermentrout 1989; St-Hilaire and Longtin 2004; Tsumoto et al. 2006). First, we employ the dynamic state feedback control law of Nguyen and Hong (2012) to relocate two Hopf bifurcation points in the ML neuron model with Type II excitability to new desired locations to avoid their appearance in a certain range of applied current. Interestingly, not only is the aforementioned control objective achieved, but also the originally subcritical Hopf bifurcation that corresponds to the transition from quiescence to periodic spiking will become supercritical. Hence, the jumping behavior that occurs when a neuron transits from quiescence to periodic spiking can be prevented. Second, we apply the proposed bifurcation control method to change the types of neuronal excitability. Specifically, we transform Type I excitability into Type II excitability by creating a new Hopf bifurcation at a preferable value of the applied current such that the neuron undergoes a Hopf bifurcation (instead of a SNIC bifurcation) from quiescence to periodic spiking.

The rest of this paper is organized as follows. In Sect. 2, we briefly describe the ML neuron model. The excitability and bifurcations of the ML neuron model are also reviewed in this section. In Sect. 3, we first state the conditions for the emergence of Hopf bifurcations. Then a closed-loop ML system based on a dynamic state feedback control law is proposed. The details of control objectives as well as the procedure to obtain the control gains are fully addressed in this section. Finally, conclusions are given in Sect. 4.

2 ML model and its dynamics

2.1 Model description

The ML neuron model was originally postulated to describe a variety of oscillatory membrane potential patterns of barnacle muscle fibers (Morris and Lecar 1981). This model consists of two ordinary differential equations as follows:

$$\dot{V} = \frac{1}{C}\{I - \bar{g}_{\mathrm{K}} w(V - V_{\mathrm{K}}) - \bar{g}_{\mathrm{Ca}} m_{\infty}(V)(V - V_{\mathrm{Ca}}) - \bar{g}_{\mathrm{L}}(V - V_{\mathrm{L}})\}, \quad (1)$$

$$\dot{w} = \phi \frac{w_\infty(V) - w}{\tau_w(V)}, \tag{2}$$

where V is the membrane potential, w is the recovery variable associated with the slow ionic potassium current, C is the membrane capacitance, and I is the external applied current. The reversal potentials of the potassium, calcium, and leak currents are denoted by V_K, V_{Ca}, and V_L, respectively. The maximum conductances of the corresponding ionic currents are denoted by $\bar{g}_K$, $\bar{g}_{Ca}$, and $\bar{g}_L$, and, finally, ϕ is the temperature factor.

The calcium current is assumed to have an instantaneous response. Therefore, the activation gating variable of the calcium ion channel is approximated by its steady-state value m_∞. For the barnacle muscle fiber, the voltage-dependent $m_\infty(V)$ is given by

$$m_\infty(V) = 0.5\,[1 + \tanh\{(V - V_1)/V_2\}], \tag{3}$$

where V_1 and V_2 are the constant potentials. The steady-state value of the recovery variable w_∞ and the time constant τ_w with respect to the potassium activation are also voltage-dependent functions, which are defined as follows:

$$w_\infty(V) = 0.5\,[1 + \tanh\{(V - V_3)/V_4\}], \tag{4}$$

$$\tau_w(V) = 1/\cosh\{(V - V_3)/(2V_4)\}, \tag{5}$$

where V_3 and V_4 are constant potentials.

2.2 Excitability and bifurcations in the ML neuron model

The ML neuron model can exhibit properties of either Type I excitability or Type II excitability depending on two different sets of parameter values (Rinzel and Ermentrout 1989; Tsumoto et al. 2006). In these two sets, except for V_3, V_4, $\bar{g}_{Ca}$, and ϕ, the parameter values are the same $-V_K = -84\,\text{mV}$, $V_{Ca} = 120\,\text{mV}$, $V_L = -60\,\text{mV}$, $\bar{g}_K = 8.0\,\text{mS/cm}^2$, $\bar{g}_L = 2.0\,\text{mS/cm}^2$, $C = 20\,\mu\text{F/cm}^2$, $V_1 = -1.2$, and $V_2 = 18\,\text{mV}$.

Case 1: Type I excitability where $V_3 = 12\,\text{mV}$, $V_4 = 17.4\,\text{mV}$, $\bar{g}_{Ca} = 4\,\text{mS/cm}^2$, and $\phi = 1/15$. The f–I curve of this case is shown in Fig. 1. It can be seen that initially the slope of the f–I curve tends to infinity; therefore, the neuron starts firing with an arbitrary low frequency. The firing frequency increases continuously with the increase in the applied current over a wide range. The bifurcation diagram of the membrane potential V versus the applied current I is depicted in Fig. 2. Here, the thick solid lines represent stable equilibrium points, whereas the dotted line represents unstable ones. The maxima and minima of stable and unstable limit cycles are indicated by thin and dashed lines, respectively. Note that all the bifurcation diagrams in this paper were produced using the XPPAUT software package (Ermentrout 2002). Evidently, the neuron undergoes a SNIC bifurcation of the equilibrium, which leads to a periodic spiking state at $I = 39.96\,\mu\text{A/cm}^2$, and the periodic oscillation terminates with the appearance of a saddle-node bifurcation of the spiking attractor at $I = 116.1\,\mu\text{A/cm}^2$. Also, a subcritical Hopf bifurcation of the equilibrium is observed at $I = 97.82\,\mu\text{A/cm}^2$.

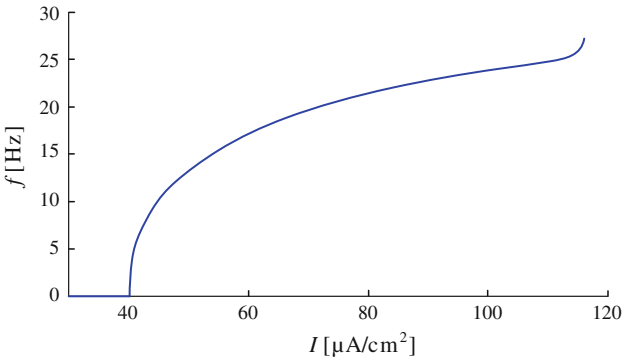

Fig. 1 f–I curve of original ML neuron model with Type I excitability, which shows the neuron starting to fire at an arbitrary low frequency

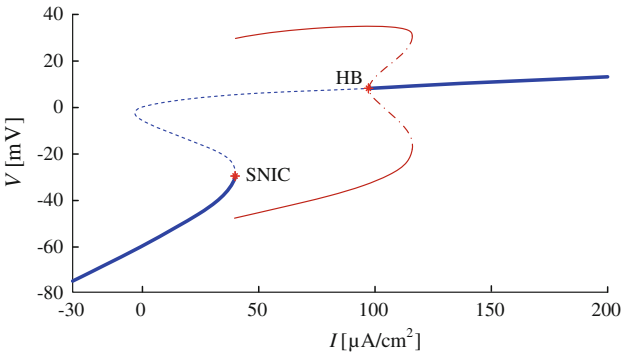

Fig. 2 Bifurcation diagram of original ML neuron model with Type I excitability (*thick solid lines*: stable equilibria; *dotted line*: unstable ones; *thin* and *dashed lines*: maxima and minima of stable and unstable limit cycles, respectively)

Case 2: Type II excitability where $V_3 = 2\,\text{mV}$, $V_4 = 30\,\text{mV}$, $\bar{g}_{Ca} = 4.4\,\text{mS/cm}^2$, and $\phi = 1/25$. In this case, the f–I curve is discontinuous, which shows the neuron starting to fire at a nonzero frequency (about 7 Hz), and the response frequency range is narrow (Fig. 3). The bifurcation diagram of the membrane potential V as a function of the applied current I is shown in Fig. 4. From Fig. 4 it can be seen that the neuron undergoes a subcritical Hopf bifurcation of the equilibrium, which leads to a periodic spiking at $I = 93.86\,\mu\text{A/cm}^2$, and the periodic oscillation terminates with the appearance of a saddle-node bifurcation of the spiking attractor at $I = 216.9\,\mu\text{A/cm}^2$. Another subcritical Hopf bifurcation of the equilibrium is identified at $I = 212\,\mu\text{A/cm}^2$.

On the basis of the foregoing analyses we can verify that the type of bifurcation determines the type of neuronal excitability in a given model (Rinzel and Ermentrout 1989;

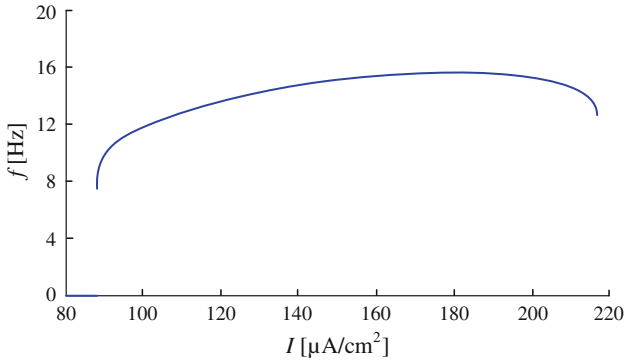

Fig. 3 f–I curve of original ML neuron model with Type II excitability, which shows the neuron starting to fire with a nonzero frequency

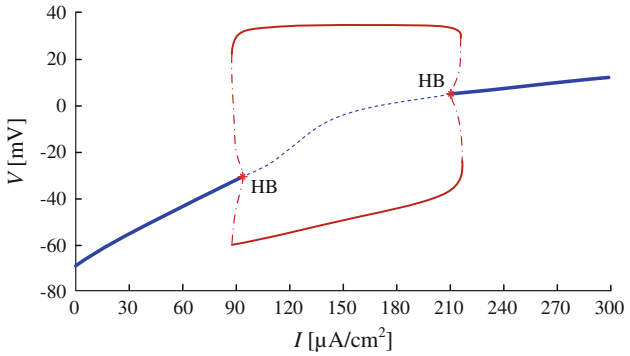

Fig. 4 Bifurcation diagram of original ML neuron model with Type II excitability (*lines* have same meanings as in Fig. 2)

Izhikevich 2007). In particular, a neuron with Type I excitability undergoes a SNIC bifurcation, whereas a neuron with Type II excitability undergoes a Hopf bifurcation from the resting state to a periodic spiking state.

3 Hopf bifurcation control of ML neuron model

3.1 Conditions for emergence of Hopf bifurcations

Consider the following n-dimensional nonlinear system:

$$\dot{x} = f(x, \mu),$$

$$f : R^{n+1} \to R^n, x \in R^n, \mu \in R, \tag{6}$$

where x is the state vector and μ the bifurcation parameter; the vector field $f(x, \mu)$ is smooth in x and μ. Suppose that system (6) has an equilibrium point at $x = x^e$ for some $\mu = \mu^e$, i.e., $f(x^e, \mu^e) = 0$. The conditions under which system (6) undergoes a Hopf bifurcation at $\mu = \mu^e$ are as follows: (1) the Jacobian matrix of system (6) evaluated at the equilibrium point has a pair of pure imaginary eigenvalues $\lambda(\mu^e) = \pm j\omega$, while the other eigenvalues have negative real parts; and (2) the eigenvalues $\lambda(\mu^e)$ cross the imaginary axis at some nonzero speed at the bifurcation point. The former condition is known as the eigenvalue crossing condition, whereas the latter condition is known as the transversality condition. In creating a Hopf bifurcation at a desired parameter value using a control signal, one expects to obtain the analytical expressions of all the eigenvalues of the Jacobian matrix of a closed-loop control system as functions of the control gains. However, for a high-dimensional system, such analytical expressions are very difficult or even impossible to obtain. To avoid directly solving for all the eigenvalues, we adopt the equivalent conditions for the emergence of Hopf bifurcations (Liu 1994). The main idea is based on the Routh–Hurwitz stability criterion, by which the eigenvalue crossing condition demands that all the coefficients of the characteristic polynomial, as well as the first $(n-2)$ Routh–Hurwitz determinants, be positive, while the transversality condition requires that the $(n-1)$th Routh–Hurwitz determinant change from positive to negative at a nonzero rate. The equivalent conditions in Liu (1994) are summarized as follows.

Let the characteristic polynomial of the Jacobian matrix be

$$P(\lambda; \mu^e) = p_0(\mu^e)\lambda^n + p_1(\mu^e)\lambda^{n-1} + \cdots + p_n(\mu^e). \tag{7}$$

The following matrix is introduced:

$$H_n(\mu^e) = \begin{bmatrix} p_1(\mu^e) & p_0(\mu^e) & 0 & \cdots & 0 \\ p_3(\mu^e) & p_2(\mu^e) & p_1(\mu^e) & \cdots & 0 \\ p_5(\mu^e) & p_4(\mu^e) & p_3(\mu^e) & \cdots & 0 \\ \vdots & \vdots & \vdots & \ddots & \vdots \\ p_{2n-1}(\mu^e) & p_{2n-2}(\mu^e) & p_{2n-3}(\mu^e) & \cdots & p_n(\mu^e) \end{bmatrix}, \tag{8}$$

where $p_i(\mu^e) = 0$ if $i < 0$ or $i > n$. Let

$$\Delta_1(\mu^e) = p_1(\mu^e), \tag{9}$$

$$\Delta_2(\mu^e) = \begin{vmatrix} p_1(\mu^e) & p_0(\mu^e) \\ p_3(\mu^e) & p_2(\mu^e) \end{vmatrix},$$

$$\vdots$$

$$\Delta_{n-1}(\mu^e) = \begin{vmatrix} p_1(\mu^e) & p_0(\mu^e) & 0 & \cdots & 0 \\ p_3(\mu^e) & p_2(\mu^e) & p_1(\mu^e) & \cdots & 0 \\ p_5(\mu^e) & p_4(\mu^e) & p_3(\mu^e) & \cdots & 0 \\ \vdots & \vdots & \vdots & \ddots & \vdots \\ p_{2n-3}(\mu^e) & p_{2n-4}(\mu^e) & p_{2n-5}(\mu^e) & \cdots & p_{n-1}(\mu^e) \end{vmatrix}$$

Then system (6) undergoes a Hopf bifurcation at $\mu = \mu^e$ if the following conditions are satisfied.

(H1) Eigenvalue crossing condition:

$$p_n(\mu^e) > 0, \tag{10}$$

$$\Delta_i(\mu^e) > 0, \quad i = 1, \ldots, n-2, \tag{11}$$

$$\Delta_{n-1}(\mu^e) = 0. \tag{12}$$

(H2) Transversality condition:

$$\frac{d\{\Delta_{n-1}(\mu)\}}{d\mu}\Big|_{\mu=\mu^e} \neq 0. \tag{13}$$

3.2 Closed-loop ML system based on a dynamic state feedback controller

A general dynamic state feedback control law for controlling Hopf bifurcations in system (6) is introduced as follows:

$$u = u(x, y), \tag{14}$$
$$\dot{y} = g(x, y), \tag{15}$$

where $y \in R^m (1 \leq m \leq n)$ is the state vector of the controller, and the feedback control $u(x, y)$ and the vector field $g(x, y)$ are smooth in x and y. Specifically, the following feedback control law, which has a linear term and a cubic term, is proposed (Nguyen and Hong 2012).

$$u_i(x_i, y_i) = k_{1i}x_i + k_{3i}(x_i - x_i^{e1})^3 - l_i y_i, \tag{16}$$
$$\dot{y}_i = u_i(x_i, y_i), \tag{17}$$

where x_i^{e1} $(i = 1, 2, \ldots, m)$ are the equilibrium values of x_i at the first designated Hopf bifurcation point, k_{1i} and k_{3i} are the control gains, and l_i are constant parameters. Then the closed-loop control system can be written as

$$\dot{x} = f(x, \mu) + u(x, y), \tag{18}$$
$$\dot{y} = g(x, y), \tag{19}$$

where $u(x, y) = [u_1(x_1, y_1), \ldots, u_m(x_m, y_m), 0, \ldots, 0]^T$ and $g(x, y) = [u_1(x_1, y_1), \ldots, u_m(x_m, y_m)]^T$. Due to the nature of the proposed control law in (16)–(17), $u_i = 0$ for $\dot{y}_i = u_i = 0$. Hence, if x^e is an equilibrium of the original system (6), then (x^e, y^e) is the equilibrium of the control system (18)–(19), where $y^e = (y_1^e, y_2^e, \ldots, y_m^e)$ and $y_i^e = (k_{1i}x_i^e + k_{3i}(x_i^e - x_i^{e1})^3)/l_i$ $(i = 1, 2, \ldots, m)$. In other words, all the equilibrium points of the original system (6) remain unchanged when the control law (16)–(17) is applied. The ability to preserve the equilibrium structure of the original system during the control process is one of the essential characteristics required in bifurcation control. In this paper, we select only the membrane potential V as an input to be controlled because it can be readily measured, and therefore the controller can be realized easily. Then, the closed-loop ML system is given as follows:

$$\dot{V} = \frac{1}{C}\{I - \bar{g}_K w(V - V_K) - \bar{g}_{Ca} m_\infty(V)(V - V_{Ca}) - \bar{g}_L(V - V_L)\} + k_1 V + k_3(V - V^{e1})^3 - ly, \tag{20}$$
$$\dot{w} = \phi\frac{w_\infty(V) - w}{\tau_w(V)}, \tag{21}$$
$$\dot{y} = k_1 V + k_3(V - V^{e1})^3 - ly, \tag{22}$$

where V^{e1} is the equilibrium value of the membrane potential at the first designated Hopf bifurcation.

3.3 Relocate the inherent Hopf bifurcations

In this section, we employ the proposed control law (16)–(17) to relocate both inherent Hopf bifurcations in the ML model with Type II excitability (Fig. 4) to the desired points to avoid their occurrence in a certain range of applied current, irrespective of whether the corresponding steady states are stable or unstable. Specifically, we aim to advance the left Hopf bifurcation toward $I_1 = 60\,\mu\text{A/cm}^2$ and the right Hopf bifurcation toward $I_2 = 180\,\mu\text{A/cm}^2$. At the first designated Hopf bifurcation (i.e., $I_1 = 60\,\mu\text{A/cm}^2$), the equilibrium value of the membrane potential of the ML model with parameter values specified in case 2 of Sect. 2.2 is obtained as $V^{e1} = -36.7547\,\text{mV}$. Here, we set $l = 0.2$. Therefore, the control law in this case can be written as

$$u(V, y) = k_1 V + k_3(V + 36.7574)^3 - 0.2y, \tag{23}$$
$$\dot{y} = k_1 V + k_3(V + 36.7574)^3 - 0.2y. \tag{24}$$

In what follows, we will show how to determine the control gains k_1 and k_3 such that the closed-loop control system (20)–(22) undergoes Hopf bifurcations at $I_1 = 60\,\mu\text{A/cm}^2$ and $I_2 = 180\,\mu\text{A/cm}^2$.

At $I_1 = 60\,\mu\text{A/cm}^2$, the equilibrium point of (20)–(22) is obtained as $(V^{e1}, w^{e1}, y^{e1}) = (-36.7547, 0.0702, -183.7735k_1)$. Therefore, we obtain the Jacobian matrix as follows:

$$J(I_1) = \begin{bmatrix} -0.0612 + k_1 & -18.8981 & -0.2 \\ 0.0002 & -0.0486 & 0 \\ k_1 & 0 & -0.2 \end{bmatrix}. \tag{25}$$

Then the characteristic polynomial of $J(I_1)$ is given by

$$P(\lambda; I_1) = p_0\lambda^3 + p_1\lambda^2 + p_2\lambda + p_3 = 0, \tag{26}$$

where $p_0 = 1$, $p_1 = 0.3099 - k_1$, $p_2 = 0.0289 - 0.0486k_1$, and $p_3 = 0.0014$.

Substituting $p_i, i = 0, 1, \ldots, 3$, into the eigenvalue crossing condition (10)–(12) we obtain

$$p_3 = 0.0014 > 0, \tag{27}$$
$$\Delta_1 = p_1 = 0.3099 - k_1 > 0, \tag{28}$$
$$\Delta_2 = p_1 p_2 - p_0 p_3 = 0.0486 - k_1^2 - 0.0440\,k_1 + 0.0076 = 0. \tag{29}$$

Solving the preceding two inequalities (27) and (29), we obtain $k_1 = 0.2311$. For the transversality condition (13) it can be numerically computed that

$$\frac{d\{\Delta_2(I)\}}{dI}\Big|_{I=I_1} = -0.6041 \times 10^{-4} \neq 0. \tag{30}$$

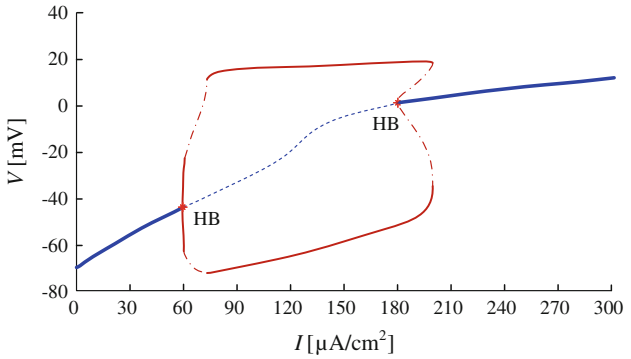

Fig. 5 Bifurcation diagram of closed-loop ML system: two inherent Hopf bifurcations in original ML model with Type II excitability (Fig. 4) have been relocated to new positions under control law in (23)–(24) with $k_1 = 0.2311$ and $k_3 = -1.3539 \times 10^{-4}$ (*lines* have same meanings as in Fig. 2)

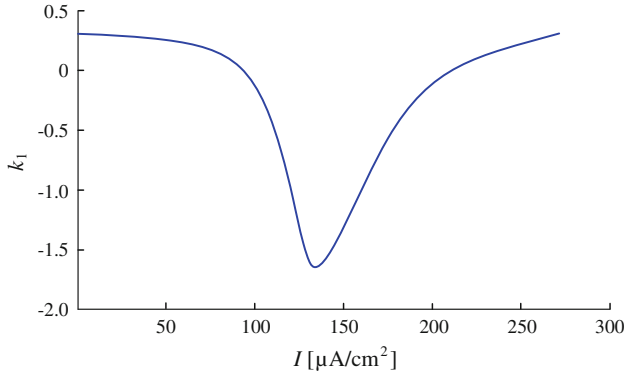

Fig. 6 Two-parameter bifurcation diagram depicting continuation of Hopf bifurcation points of closed-loop ML system with respect to k_1 when $k_3 = 0$ (the left and right Hopf bifurcation points are depicted by left and right branches, respectively)

From the preceding calculation it is noted that k_3 has no effect on the location of the left Hopf bifurcation point. Therefore, k_3 can be used to relocate the right Hopf bifurcation point. The equilibrium point of the closed-loop ML system (20)–(22) at $I_2 = 180\,\mu\text{A/cm}^2$ is obtained as $(V^{e2}, w^{e2}, y^{e2}) = (4.4440, 0.5406, 5.1352 + 349641k_3)$. Substituting the obtained value of k_1 into the Jacobian matrix of the closed-loop control system gives us

$$J(I_2) = \begin{bmatrix} 0.4125 + 5092k_3 & -35.3776 & -0.2 \\ 6.6281 \times 10^{-4} & -0.0401 & 0 \\ 0.2311 + 5092k_3 & 0 & -0.2 \end{bmatrix}. \quad (31)$$

The characteristic polynomial of $J(I_2)$ is given as follows:

$$P(\lambda; I_2) = p_0\lambda^3 + p_1\lambda^2 + p_2\lambda + p_3 = 0, \quad (32)$$

where $p_0 = 1$, $p_1 = -0.1724 - 5092k_3$, $p_2 = -0.0213 - 203.8495k_3$, and $p_3 = 0.0032$. According to the conditions for the emergence of Hopf bifurcations formulated in (10)–(13), we finally obtain $k_3 = -1.3539 \times 10^{-4}$.

The bifurcation diagram of the controlled ML system is depicted in Fig. 5. As expected, the left and right Hopf bifurcation points have been successfully advanced toward $I_1 = 60\,\mu\text{A/cm}^2$ and $I_2 = 180\,\mu\text{A/cm}^2$, respectively. It is interesting that the left Hopf bifurcation in the controlled ML system becomes supercritical. Therefore, the occurrence of jumping behavior between quiescence and periodic spiking in the controlled ML system under perturbation is prevented.

To convey more of the effect of the control gains k_1 and k_3 on the locations of Hopf bifurcation points in the closed-loop ML system (20)–(22), two-parameter bifurcation diagrams with respect to k_1 and k_3 are presented. As mentioned previously, k_3 has no effect on the location of the left Hopf bifurcation point. Therefore, we temporally set $k_3 = 0$ and vary the control gain k_1. In this case, changes to the Hopf bifurcation points are shown in Fig. 6, in which the left branch shows a continuation of the left Hopf bifurcation point and the right branch depicts a continuation of the right Hopf bifurcation point. It can be seen that when varying the control gain k_1, not only does the location of the left Hopf bifurcation point change, but that of the right Hopf bifurcation point does as well. Decreasing the value of k_1 results in a decrease in the distance between two Hopf bifurcation points. These two Hopf bifurcation points approach each other when $k_1 = -1.6382$, corresponding to the value $I = 136\,\mu\text{A/cm}^2$. With further decreases in k_1, a Hopf bifurcation no longer occurs; therefore, the neuron cannot fire spikes. From Fig. 6 it is obvious that one can relocate the left Hopf bifurcation point to any location in the region $0 \le I < 136\,(\mu\text{A/cm}^2)$ by selecting the appropriate value of k_1 in the region $0.2972 \le k_1 < -1.6382$.

Once the location of the left Hopf bifurcation point is determined by a specific value of k_1, the location of the right Hopf bifurcation can be relocated to a desired location through the control gain k_3. To show the changes in the right Hopf bifurcation point location due to k_3, we fix the left Hopf bifurcation point at $I = 60\,\mu\text{A/cm}^2$ (i.e., $k_1 = 0.2311$ and $V^{e1} = -36.7574$) and create the two-parameter bifurcation diagram with respect to k_3, which shows the continuation of the right Hopf bifurcation point. As shown in Fig. 7, the location of the right Hopf bifurcation point can be assigned within a wide range of the applied current.

3.4 Changing the types of neuronal excitability

As mentioned in Sect. 2.2, the ML neuron model can exhibit properties of either Type I excitability or Type II excitability depending on two different sets of values of four parameters, namely, V_3, V_4, $\bar{g}_{\text{Ca}}$, and ϕ. In other words, to change the types of neuronal excitability, one must change the values of these parameters. From a dynamical point of view, Type I excitability undergoes a SNIC bifurcation, while Type II excitability undergoes a Hopf bifurcation from quiescence

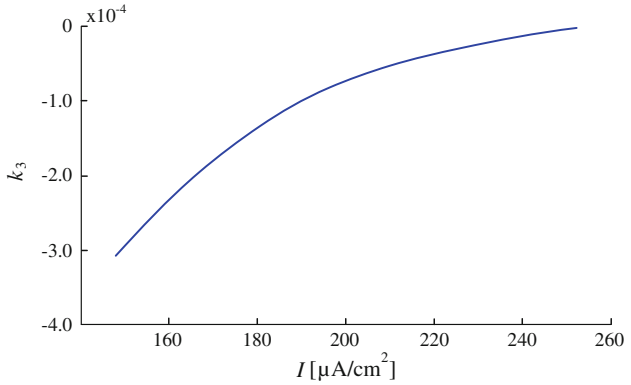

Fig. 7 Two-parameter bifurcation diagram that shows continuation of right Hopf bifurcation point of closed-loop ML system with respect to k_3 when left Hopf bifurcation point is fixed at $I = 60\,\mu\text{A/cm}^2$ (i.e., $k_1 = 0.2311$ and $V^{e1} = -36.7574$)

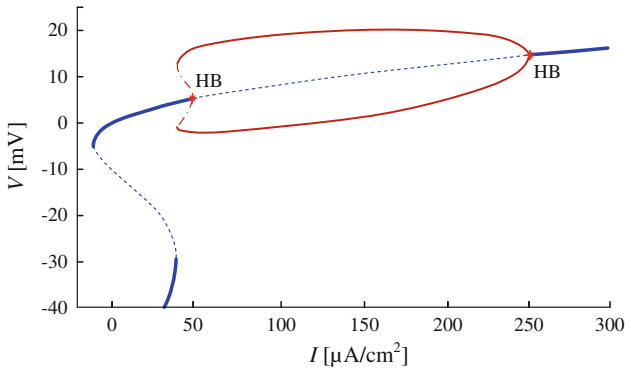

Fig. 8 Bifurcation diagram of closed-loop ML system: the neuron transits from quiescence to periodic spiking via Hopf bifurcation instead of SNIC bifurcation (Fig. 2) under the control law in (33)–(34) with $k_1 = 0.3395$ and $k_3 = -0.1997 \times 10^{-2}$ (definitions of individual *lines* are as in Fig. 2)

to periodic spiking. Therefore, by modifying the bifurcation structure one may change the types of neuronal excitability. In this section, we employ the proposed bifurcation control method to convert Type I excitability into Type II excitability without changing any parameter values. The idea is to create two Hopf bifurcation points at desired parameter values such that the neuron transits from quiescence to periodic spiking via a Hopf bifurcation (instead of a SNIC bifurcation) and the periodic oscillation terminates at another Hopf bifurcation. The original bifurcation diagram of the ML model with Type I excitability is shown in Fig. 2. At first, we shift the inherent Hopf bifurcation to $I_1 = 250\,\mu\text{A/cm}^2$, and then a new Hopf bifurcation is created at $I_2 = 50\,\mu\text{A/cm}^2$. At $I_1 = 250\,\mu\text{A/cm}^2$, the equilibrium value of the membrane potential of the ML model with parameter values specified in case 1 of Sect. 2.2 is obtained as $V^{e1} = 14.8798\,\text{mV}$. Therefore, the control law in this case is written as follows:

$$u(V, y) = k_1 V + k_3 (V - 14.8798)^3 - 0.2y, \tag{33}$$

$$\dot{y} = k_1 V + k_3 (V - 14.8798)^3 - 0.2y. \tag{34}$$

Then the Jacobian matrix of the closed-loop control system (20)–(22) can be obtained as follows:

$$J(I_1) = \begin{bmatrix} -0.2170 + k_1 & -39.5519 & -0.2 \\ 0.0019 & -0.0669 & 0 \\ k_1 & 0 & -0.2 \end{bmatrix}, \tag{35}$$

and the characteristic polynomial of $J(I_1)$ is

$$P(\lambda; I_1) = p_0\lambda^3 + p_1\lambda^2 + p_2\lambda + p_3 = 0, \tag{36}$$

where $p_0 = 1$, $p_1 = 0.4839 - k_1$, $p_2 = 0.1453 - 0.0669k_1$, and $p_3 = 0.0177$. The substitution of p_i ($i = 0 \sim 3$) to (10)–(13) yields $k_1 = 0.3395$.

Substituting the obtained value of k_1 into the Jacobian matrix of the closed-loop control system (20)–(22), at $I_2 = 50\,\mu\text{A/cm}^2$, we obtain the following expression.

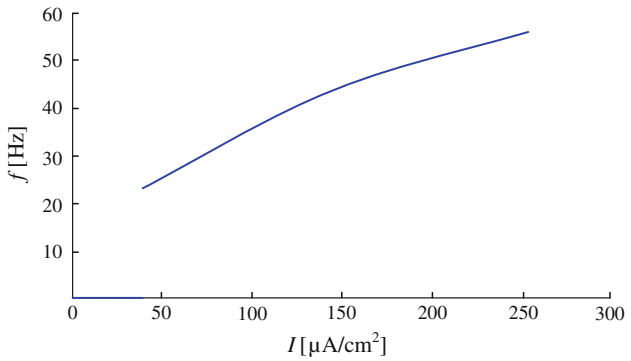

Fig. 9 f–I curve of closed-loop ML system exhibiting a discontinuity, showing that the type of neuronal excitability has been converted from Type I (Fig. 1) to Type II under the control law in (33)–(34) with $k_1 = 0.3395$ and $k_3 = -0.1997 \times 10^{-2}$

$$J(I_2) = \begin{bmatrix} 0.5328 + 266.5439k_3 & -35.7815 & -0.2 \\ 0.0017 & -0.0678 & 0 \\ 0.3395 + 266.5439k_3 & 0 & -0.2 \end{bmatrix}. \tag{37}$$

The characteristic polynomial of $J(I_2)$ becomes

$$P(\lambda; I_2) = p_0\lambda^3 + p_1\lambda^2 + p_2\lambda + p_3 = 0, \tag{38}$$

where $p_0 = 1$, $p_1 = -0.2649 - 266.5439k_3$, $p_2 = -4.82 \times 10^{-4} - 18.0849k_3$, and $p_3 = 0.0095$. Finally, we obtain $k_3 = -0.1997 \times 10^{-2}$. The bifurcation diagram of the controlled ML system is shown in Fig. 8. It is obvious that the neuron transits from quiescence to periodic spiking via a Hopf bifurcation instead of a SNIC bifurcation as the uncontrolled system does (Fig. 2). The firing frequency versus the applied current is depicted in Fig. 9. It can be seen that the f–I curve is discontinuous; the neuron starts firing with a nonzero frequency. Therefore, under control, the type of neuronal excitability has been changed from Type I to Type II.

4 Conclusions

Our attention in this paper focused on addressing the problem of controlling bifurcations in the ML neuron model. Using a dynamic state feedback control law, the locations of both Hopf bifurcations in the ML neuron model with Type II excitability could be relocated, simultaneously, to new desired parameter values. In addition, for the ML neuron model originally exhibiting properties of Type I excitability, if a new Hopf bifurcation was created at a preferable value of the stimulated current, the type of neuronal excitability could be transformed from Type I excitability to Type II excitability without changing any parameter values of the neuron model. Bifurcation phenomena are believed to play an important role in the emergence of many neurological diseases such as epilepsy, Parkinson's disease, and others. Therefore, we expect that the results obtained in this paper will lead to new treatment strategies for neurological diseases.

Acknowledgments This research was supported by the World Class University program through the National Research Foundation of Korea funded by the Ministry of Education, Science and Technology, Republic of Korea (Grant No. R31-20004).

References

Abed EH, Fu JH (1986) Local feedback stabilization and bifurcation control: 1-Hopf bifurcation. Syst Control Lett 7(1):11–17

Abed EH, Wang HO (1995) Feedback control of bifurcation and chaos in dynamical systems. In: Kliemann W, Sri Namachchivaya N (eds) Nonlinear dynamics and stochastic mechanics. CRC Press, Boca Raton, pp 153–173

Asai Y, Nomura T, Sato S, Tamaki A, Matsuo Y, Mizukura I, Abe K (2003) A coupled oscillator model of disordered interlimb coordination in patients with Parkinson's disease. Biol Cybern 88(2):152–162

Berns DW, Moiola JL, Chen G (1998) Feedback control of limit cycle amplitudes from a frequency domain approach. Automatica 34(12):1567–1573

Brandt ME, Chen G (1997) Bifurcation control of two nonlinear models of cardiac activity. IEEE Trans Circuits Syst I 44(10):1031–1034

Brown E, Moehlis J, Holmes P (2004) On the phase reduction and response dynamics of neural oscillator populations. Neural Comput 16(4):673–715

Bélair J, Glass L, van der Heiden U, Milton J (1995) Dynamical diseases: identification, temporal aspects and treatment strategies of human illnesses. Chaos 5(1):1–7

Chen G, Moiola JL, Wang HO (2000) Bifurcation control: theories, methods, and applications. Int J Bifur Chaos 10(3):511–548

Ding L., Hou C. (2010) Stabilizing control of Hopf bifurcation in the Hodgkin–Huxley model via washout filter with linear control term. Nonlinear Dyn 60(1–2):131–139

Ermentrout B (2002) Simulating, analyzing, and animating dynamical systems: a guide to XPPAUT for researchers and students. SIAM, Philadelphia

Hodgkin AL (1948) The local electric changes associated with repetitive action in a non-medullated axon. J Physiol 107(2):165–181

Izhikevich EM (2000) Neuronal excitability, spiking and bursting. Int J Bifur Chaos 10(6):1171–1266

Izhikevich EM (2007) Dynamical systems in neuroscience. MIT Press, Cambridge

Kang W (1998) Bifurcation and normal form of nonlinear control systems, part I. SIAM J Control Optim 36(1):193–212

Kramer MA, Lopour BA, Kirsch HE, Szeri AJ (2006) Bifurcation control of a seizing human cortex. Phys Rev E 73(4):041928

Laing CR, Longtin A (2003) Periodic forcing of a model sensory neuron. Phys Rev E 67(5):051928

Lefebvre J, Longtin A, LeBlanc VG (2009) Dynamics of driven recurrent networks of ON and OFF cells. Phys Rev E 80(4):041912

Liu WM (1994) Criterion of Hopf bifurcations without using eigenvalues. J Math Anal Appl 182(1):250–256

Luo M, Wu Y, Peng J (2009) Washout filter aided mean field feedback desynchronization in an ensemble of globally coupled neural oscillators. Biol Cybern 101(3):241–246

Mackey MC, van der Heiden U (1982) Dynamical diseases and bifurcations: understanding functional disorders in physiological systems. Funkt Biol Med 1(156):156–164

Morris C, Lecar H (1981) Voltage oscillations in the Barnacle giant muscle fiber. Biophys J 35(1):193–213

Nguyen LH, Hong KS (2011) Synchronization of coupled chaotic FitzHugh–Nagumo neurons via Lyapunov functions. Math Couput Simul 82(4):590–603

Nguyen LH, Hong KS (2012) Hopf bifurcation control via a dynamic state-feedback control. Phys Lett A 376(4):442–446

Rinzel J, Ermentrout GB (1989) Analysis of neural excitability and oscillations. In: Koch CH, Segev I (eds) Methods in neuronal modeling from synapses to networks. MIT Press, Cambridge, pp 135–169

St-Hilaire M, Longtin A (2004) Comparison of coding capabilities of type I and type II neurons. J Comput Neurosci 16(3):299–313

Tesi A, Abed EH, Genesio R, Wang HO (1996) Harmonic balance analysis of period-doubling bifurcations with implications for control of nonlinear dynamics. Automatica 32(9):1255–1271

Titcombe MS, Glass L, Guehl D, Beuter A (2001) Dynamics of Parkinsonian tremor deep brain stimulation. Chaos 11(4):766–773

Touboul J, Brette R (2008) Dynamics and bifurcations of the adaptive exponential integrate-and-fire model. Biol Cybern 99(4–5):319–334

Tsumoto K, Kitajima H, Yoshinaga T, Aihara K, Kawakami H (2006) Bifurcations in Morris–Lecar neuron model. Neurocomputing 69(4–6):293–316

Wang HO, Abed EH (1995) Bifurcation control of a chaotic system. Automatica 31(9):1213–1226

Wen G, Xu D (2005) Control algorithm for creation of Hopf bifurcation in continuous-time systems of arbitrary dimension. Phys Lett A 337(1–2):93–100

Xiao M, Cao J (2007) Delayed feedback-based bifurcation control in an Internet congestion model. J Math Anal Appl 332(2):1010–1027

Xie Y, Aihara K, Kang Y.M. (2008a) Change in types of neuronal excitability via bifurcation control. Phys Rev E 77(2):021917

Xie Y, Chen L, Kang YM, Aihara K (2008b) Controlling the onset of Hopf bifurcation in the Hodgkin–Huxley model. Phys Rev E 77(6):061921

Yu P, Chen G (2004) Hopf bifurcation control using nonlinear feedback with polynomial functions. Int J Bifur Chaos 14(5):1683–1704